Fault Tolerant Actuation of a Railway Track Switch: a Simulation Study

Linxiao Li, Saikat Dutta, Roger Dixon and Edward Stewart

Abstract— Track switches (also known as "point" or "turn-out") are essential to the railway system and provide route flexibility by allowing vehicles to move between tracks on the network. However, the single actuators in the current switch technology mean that a single actuator fault will result in the failure of the switch (and the concomitant delays to trains waiting to pass the switch). This paper focuses on providing redundant actuation through an approach known as High Redundancy Actuation (HRA), which might allow track switches to remain operational after failure in actuator elements. The paper also proposes the use of closed-loop control (track switches are usually operated open-loop). In the paper, we introduce a model of a C-type switch and validate it against results from a previous paper. This model is then used combined with an HRA of nine elements (3x3). Two closed-loop controllers are then proposed for each of the single actuator and the HRA actuator system. The findings indicate that closed-loop control on its own has some benefits. However, when combined with HRA, the resulting system is able to tolerate a number of faults in the actuator subsystems, creating an effective graceful degradation rather than the sudden failure with a traditional single actuator.

Index Terms— High redundancy actuator, railway track switch, fault-tolerant control, MATLAB/Simulink.

I. INTRODUCTION

Track switches (also known as "points" or "turn-outs") are key elements of the railway track, which allow vehicles to switch from one route to another. They are often driven by electric or hydraulic actuators [1]. Except for the track faults, switch faults are the most serious problem incurring the economic loss and train delay, around 13% of maintenance costs are related to turnouts [2]. Therefore, track switches are a critical single point of failure on the railway network with most current research focused on monitoring to rectify and prevent the failure [3].

In [4], Lee et al. used the characteristic data of the selected acoustic signal to detect and classify the faults of the switch. State detection of track switches is an essential method used by the railway industry to improve the reliability of turnouts. The purpose is to predict and prevent potential failures based on monitoring its working conditions [5]. Besides, most researchers try to change existing traditional mechanical structures to avoid failures. Other research proposed a novel track switch actuation method, Repoint Light, which was demonstrated at a full-scale stage [6]. In [3], Kaijuka et al. completed the model and control of a lab demonstrator from the REPOINT Light. The experience in this field shows

L. Li, R. Dixon and E. Stewart are with the School of Engineering, University of Birmingham B15 2TT, U.K (e-mail: lxl636@student.bham.ac.uk; r.dixon@bham.ac.uk; e.j.c.stewart@bham.ac.uk).

S. Dutta is associated with Coventry University CV1 5FB, U.K (e-mail: s.dutta@bham.ac.uk).
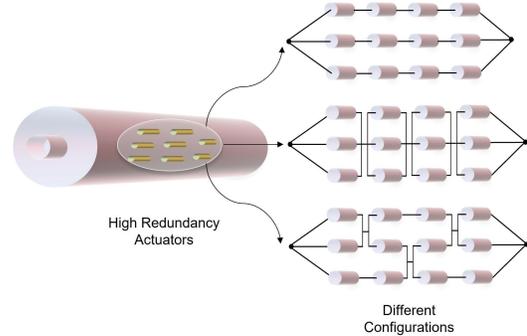
Fig. 1. Several possible configurations of the high redundancy actuator.

that alarms and warnings are primarily created after the fault occurs or is close to the fault. Although this is a valuable improvement, we argue that these solutions can only effectively keep the switch working in the face of some catastrophic failures by complete redesign of the switch.

The approach proposed here is to use the High Redundancy Actuator (HRA) concept. This is a novel method for fault-tolerant execution, which uses multiple actuation elements in series or parallel connection in the place of an individual actuator [7]. Different potential configurations of the HRA are displayed in Fig. 1. This configuration improves the reliability and availability of the actuator and provides a high degree of fault tolerance. It is noticeable that the HRA provides the benefit of shrinking size [8]. Preliminary research to date in this field has concentrated on the HRA based on electro-mechanical actuators (EMA) with a relatively small number of actuation elements. Du et al. proposed a two-by-two series-parallel HRA model and controlled it using passive fault-tolerant methods under both healthy and faulty conditions [7-9]. Another HRA with 12 EMAs was modelled and validated to compare the behaviours of the individual EMA and the HRA in open-loop and closed-loop [10]. They concluded that the HRA can still perform the expected task even though one or more sub-actuators fail. HRA has also been used for aircraft thrust reverser [11].

The actuator fault-tolerant approach not only allows continuous operation but also avoids unnecessary maintenance. The literature review identified that no fault-tolerant method has yet been developed to allow switches to operate continuously in the event of a partial failure and avoid a systemic failure. This paper aims to demonstrate HRA fault-tolerant control strategies in the reliable electro-mechanical track switches model. There are three elements: a single actuator

track switch model, HRA track switch model, and two control algorithms. The core contributions of this framework are presented.

The track switch model utilizes a finite element modelling method that does not require a co-simulation environment unlike [12], dramatically reducing the computational time without sacrificing the accuracy in Matlab/ Simulink. To the best of our knowledge, this is the first attempt to use the HRA fault-tolerant control strategy on the track switch to improve the reliability and availability. Specifically, the switch can still achieve the required task even though there is a presence of partial failures of the actuator.

II. INDIVIDUAL ACTUATOR SWITCH MODELLING

The individual actuator switch model is obtained through a physical analysis of its components. Although different switches in the installation may have different parameters, the models and interactions of the sub-components remain the same. In this paper, the switch layout and parameters of CVS C-switch (vertical shallow depth) are studied [12].
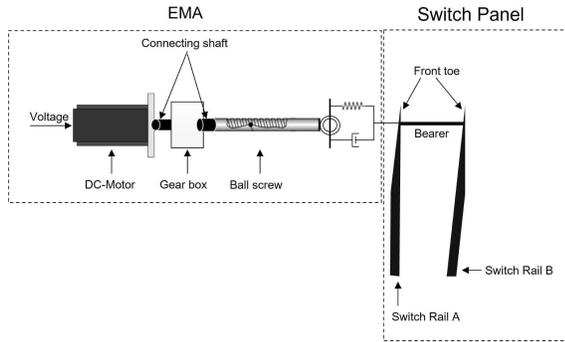
Fig. 2.   An equivalent model of the railway track switch.

A. Individual Electro-mechanical Actuator

Fig. 2 gives the individual actuator switch model structure with two main components: the electro-mechanical actuator and the switch panel model. The electro-mechanical actuator model consists of a DC motor model, a gearbox model, a mechanical linkage model, and a ball screw model. The motor drives the ball screw via the gearbox. The ball screw then converts rotary motion into linear motion. The front toe is connected with the ball screw through the mechanical linkages. The electrical equation of the DC motor is:

$$V = R_m I_m + L_m \dot{I}_m + K_e \dot{\theta} \qquad (1)$$

where R_m is the rotor resistance, I_m is the motor armature current, K_e is the back emf constant of the motor, and L_m is the rotor inductance.

The mechanical output torque T_m is defined as:

$$T_m = K_t I_m \qquad (2)$$

where K_t is the motor torque constant and I_m is the motor current.

Assuming that the ball screw and the front toe are connected by a shift spring-damper assembly. The force can be calculated by the linear motion of the ball screw and the front toe.

$$F = C_b(v_{lb} - v_{lf}) + K_b(x_{lb} - x_{lf}) \qquad (3)$$

Where, C_b and K_b are the damping and stiffness of the ball screw and front toe mechanical assembly. The linear velocities of them are v_{lb} and v_{lf}, x_{lb} and x_{lf} are the linear displacements. The purpose of the force modelling is to provide a horizontal load that applies to the rail pairs, which are explained next.

B. Switch Panel

The finite element analysis method is used to establish a rail model in Simulink [13]. The switch rail is only subjected to horizontal loads. In the classical finite element method for analysing the beam bending problem, the Hermite element is usually used [14]. Due to the characteristics of the switch rail, the cross-sectional area and moment of inertia vary with the position. Starting from the front toe, the cross-sectional area of the tip gradually widens. The cross-section area is full till the distance at point Z=5.037m away from the front toe [12]. A 3D view of a switch rail shows the change in cross-section, displayed in Fig. 3.
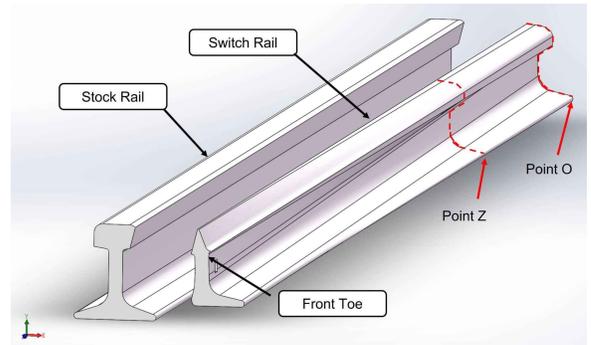
Fig. 3.   A 3D view of the switch rail and the stock rail.

The following formulas express the area A_i and moment I_i of the changed cross-section. L is the length of the switch rail and L_i represents the changeable length. The value range of the number i is from 1 to the numbers of the Hermite element, which is changeable according to a different analysis.

$$I_i = \begin{cases} I[1 - (\frac{1}{4})^2(\frac{L_i - Z}{L - Z})] & (L > L_i > Z) \\ I & (L_i \leq Z) \end{cases} \qquad (4)$$

$$A_i = \begin{cases} A[1 - (\frac{1}{4})(\frac{L_i - Z}{L - Z})] & (L > L_i > Z) \\ A & (L_i \leq Z) \end{cases} \qquad (5)$$

With the fixed cross-section at point O of the rail, the element-wise stiffness and mass matrices using Finite Elements Method are:

$$[K] = \frac{EI_i}{Le^3} \begin{bmatrix} 24 & 12Le & -12 & 6Le \\ 0 & 8Le^2 & -6Le & 2Le^2 \\ -12 & -6Le & 12 & -6Le \\ 6Le & 2Le^2 & -6Le & 4Le^2 \end{bmatrix} \qquad (6)$$

$$[M] = \frac{\rho A_i Le}{420} \begin{bmatrix} 312 & 44Le & 54 & -13Le \\ 0 & 8Le^2 & 13Le & -3Le^2 \\ 54 & 13Le & 156 & -22Le \\ -13Le & -3Le^2 & -22Le & 4Le^2 \end{bmatrix} \quad (7)$$

where E is Young's modulus, I is the moment of inertia of the cross-section, A is the area of cross-section, Le is the length of a single element.

For dynamic simulation, the damping is considered as proportional Rayleigh damping [15,16]. The full finite element system equations are:

$$[M]\ddot{\vec{X}} + [C]\dot{\vec{X}} + [K]\vec{X} = \vec{F} \quad (8)$$

$$[C] = a_0[M] + a_1[K] \quad (9)$$

where a_0 and a_1 are damping coefficient and stiffness coefficient. These values are generally derived from the experimental results in this present case, the authors find them based on the results in [12]. The parameters used for the dynamic bending formulas (4) - (9) are derived from the CVS switch layout.

The rail model is now relatively simple to implement in terms of (8) with (9), as shown in Fig. 4. In the figure, the input is the external force acting on the rail, and the output is the displacement of the node.
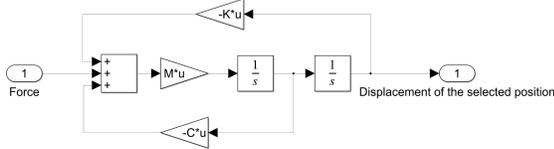
Fig. 4. The Simulink diagram of the rail model.

C. Model Validation
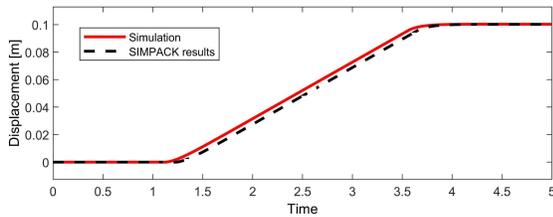
Fig. 5. Model validation for the front toe displacement.

The whole switch rail simulation model is established in MATLAB/Simulink, including an actuator and rail panel model. The model is validated by the data from the HPSS switch model built-in co-simulation of SIMPACK and Simulink [12]. The full switch system runs in the open-loop with no feedback control. The simulation results of the displacement of the front toe are illustrated in Fig. 5. The same command input pulse of a constant voltage of 120V is applied to the simulation model to move at time 1s. The simulation results show that at about 3.7s, the front toe displacement can reach 0.1m, which matches the required switch rail travel. The slight discrepancies are due to the difference in the friction coefficients between the switch rail and sleepers or other non-linearity present in the SIMPACK model. Nevertheless, the comparison between the simulation results and the available data shows that the model has a good fit. It can be concluded that the model is a good representation of the system.

III. HRA MODELLING

A track switch system with multiple actuators can be constructed by combining various sub-actuators. Here, a combination of series and parallel configuration is taken and assuming that all actuators have the same parameter value. The actuators are named and numbered with Ai for easy description (where i=1,2,...,9).

A. Actuation Configuration

In this three-by-three HRA network connecting to the front toe, three series actuators are mounted parallel in three layers. The basic components of the sub-actuators are the same as that of a single actuator. An equivalent model is in Fig. 6.
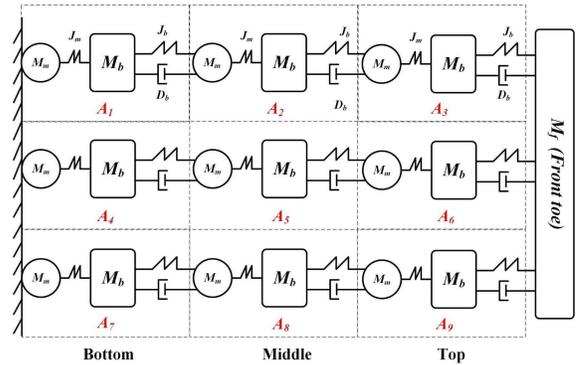
Fig. 6. An equivalent model of a three by three HRA configuration.

The entire structure encompasses three series actuators connecting in parallel. The bottom actuator (A1, A4, A7) is fixed, which acts as a load and is connected to the motor of the next actuator, and provides the position and speed information to the middle actuator (A2, A5, A8). The middle actuator (A2, A5, A8) pushes the top actuator (A3, A6, A9) which is connected with the front toe. Take the first layer as an example. The motors of A2 appears as a part of the load of the A1, the masses M_m of the motor needs to be calculated. Simultaneously, the motor of the A3 also becomes a part of the load of the A2. The other layers share the same concept. According to the newton laws, the mathematical equation for the front foe is listed below. Others are not repeated for brevity.

$$M_f X_f'' + J_b(X_f - X_{b3}) + D_b(X_f' - X_{b3}') + J_b(X_f - X_{b6}) + D_b(X_f' - X_{b6}') + J_b(X_f - X_{b9}) + D_b(X_f' - X_{b9}') = 0 \quad (10)$$

B. Fault Conditions

Two common failures are discussed here: lock-up and open circuit. Lock-up: Excessive wear of ball screw nuts may cause mechanical interference, resulting in actuator

transmission failure. In order to analyse the consequences of this fault in HRA, the fault is simulated by holding the displacement of the faulty actuator constant. Open circuit (OC): The OC failure is because of the large resistance in the circuit, which causes the DC motor not to produce current and torque. The actuator becomes "soft" and makes the actuator's force capability tend toward zero. In Simulink, this can be modelled by setting the current in the DC motor model to zero.

C. Discussion of HRA in Open Loop

The same constant voltage of 120V is applied to the HRA track switch model at time 1s. The performance of the track switch system with HRAs in the open-loop state is tested and analysed under healthy and faulty conditions. When the actuators push the front toe forward, the linear displacement of the front toe, the force, and the linear velocity are plotted in Fig. 7. Concerning the results of the HRA, the displacement and linear velocity of the single actuator have been increased by almost three times, from 0.108m to 0.323m and from 0.038m/s to 0.144m/s. The overall force is also three times than the force of a single actuator (1063N to 3188N), as expected. Here the HRA is over-sized. Note in a future study it might be required to reduce the size of the nine elements of the HRA in order to match the overall force and displacement capabilities to the desired for the switch.
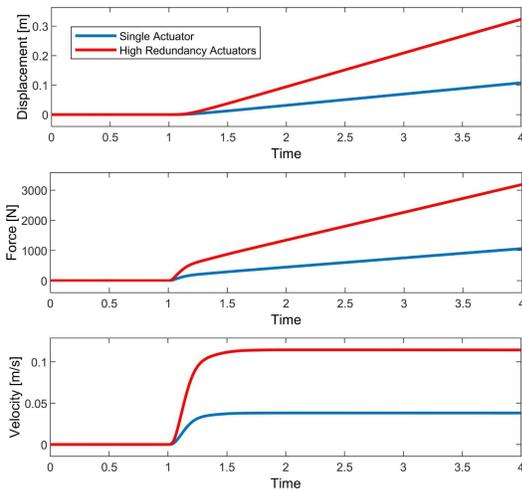
Fig. 7. The displacement, force, and velocity comparison results of the individual actuator and the HRA.

We introduce the lock-up and open circuit faults to test and analyse the 3X3 HRA structure's performance independently. The faults may emerge in any one or more of A1 to A9. Fig. 8 shows the displacement of the track switch system with HRA in single lock-up condition. It is noted that when the lock-up failure occurs in the elements connected in series simultaneously, the entire system has no output. If the lock-up faults do not wholly appear in the same row, the HRA can tolerate up to 6 locking faults. However, if the failure increases by more than six, it will immediately fail. In terms

of open-circuit faults, the HRA can tolerate up to 6, with displacements from 0.323m to 0.108m, as shown in Fig. 9. The forces also change from 3188 N to 1063 N. If there are more failures, the system is not able to complete the task of moving the switch like a single actuator.

IV. CONTROLLER DESIGN

PI controller is a successful classic control structure and is widely used in many industrial applications. However, there is little research on track switch systems. This section proposes two kinds of closed-loop controllers to control the front toe position of the single actuator track switch and the HRA track switch. Based on the operating requirements of the track switch system, the control requirements are as follows:

- To track a step in demand position without overshoot.
- Settling time < 6s;
- Rise time < 4s;
- Gain margin $\geq$ 6 dB; Phase margin $\geq$ 60 degrees.

A. Individual Controller Design

In particular, a cascaded control scheme is followed [17-19]. The designed controller includes an outer position controller for the actuator assembly and an inner controller for the motor current. The demand position is used as the outer input of the system, and the position output is regarded as the feedback to the system input as an error signal. The inner loop is designed for the motor current control. The block diagram of the PI cascaded control model is in Fig. 10. The PI controller takes the well-known form:

$$u = K_p e + K_i \int_{t_0}^{t} e dt \qquad (11)$$

K_p is the proportional gain and K_i is the integral gain, which can be obtained using the integral time constant, e is the error.

The designed cascaded controller is then applied to the track switch model. The moving switch time responses are given in Fig. 12: the front toe movement, the motor current, the voltage, the velocity of the front toe, and the power, respectively. The stabilisation times of the open-loop and the closed-loop controllers are 2.9s and 5.7s. It is also clear that the closed-loop system meets the control requirements with a rise time of 3.16s, a settling time of 5.28s, and zero overshoot. Although the rise time and settling time of closed-loop systems are slower than those from the open-loop system, the advantage of the closed-loop system is that the motor does not operate at a constant voltage input, thus reducing the power requirements during switching operations. Simultaneously, the closed-loop controller can reduce the velocity at which the front toe contacts the stock rail.

B. HRA Controller Design

Referring to Fig. 10, HRA's controller design also uses the cascaded control approach, which comprises a global position controller for the entire actuator and the local current
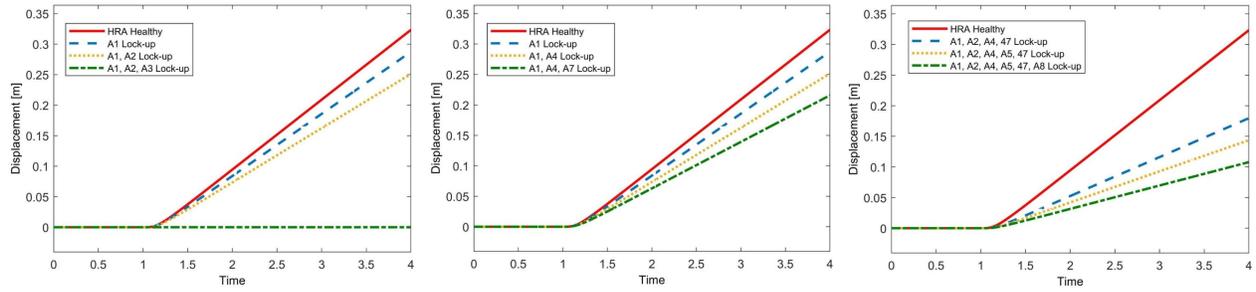
Fig. 8. The displacement comparison results of the HRA track switch with the lock-up fault.
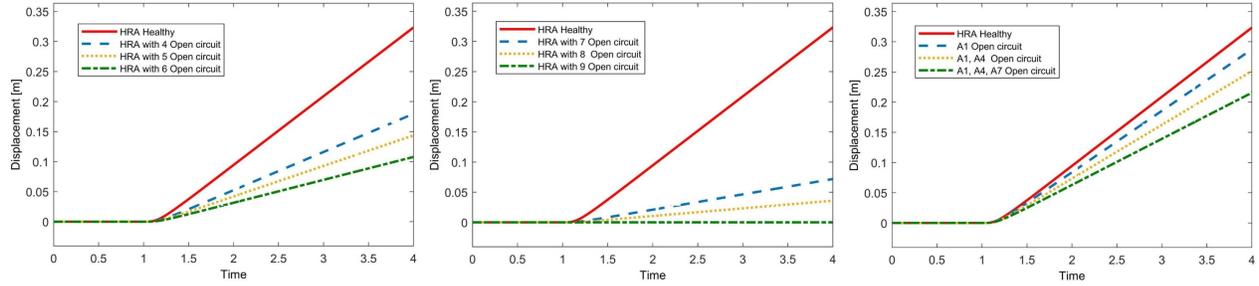
Fig. 9. The displacement comparison results of the HRA track switch with the open circuit fault.
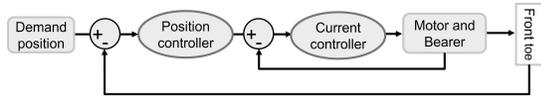
Fig. 10. Designed cascaded controller for the track switch with an individual actuator.
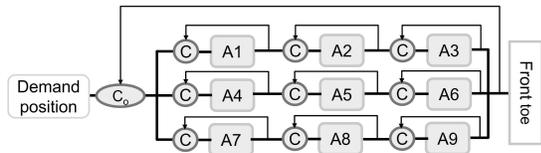
Fig. 11. Designed cascaded controller for the track switch with HRA.

Fig. 12. Comparison performance of individual actuator and HRA in open-loop and designed closed-loop system.

controllers at each sub-actuator, the details are drawn in Fig. 11. The same step signal with a 0.1m setpoint is applied as the reference.Compared with the individual actuator, the position output can reach the set requirement about 2.5 times faster. It takes less time than the open-loop. In addition to the peak voltage of 110V, the voltage input is limited at 80V, which means that when a higher gain is applied, the controller can provide a faster response. This is because the control input has not yet reached the maximum voltage that the DC motor can withstand. A third benefit is that the velocity is faster in the earlier part of the transect but is significantly lower than that of the single actuator as the switchblade approaches its desired position.

C. Comparison of Single and HRA with Faults

When one of the HRA fails, the other eight elements help overcome the failure. The same set point (0.1m) is designed as the input required to test the HRA performance

with the controller when faults occur. Fig. 13 gives the simulation results of the locked fault HRA. It can be seen that three series connection faults cause the entire HRA to fail while connecting in parallel does not produce the same result. When the four components (not in the same series) are locked, HRA is expected to continue working and fulfill the exact requirements as a single actuator. If
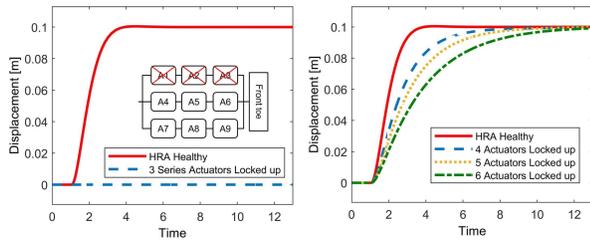
Fig. 13. Comparison results of the HRA switch model without fault and with lock-up fault.

Fig. 14. Comparison results of the HRA switch model without fault and with open-circuit fault.

more actuators are locked simultaneously, it takes longer for the system to achieve the movement task of 0.1m. Until seven actuators fail, the entire system does not generate a displacement output. For the impact of open-circuit faults on HRA, the simulation results are displayed in Fig. 14. The settling time increases with the number of actuator failures. If four elements fail in open circuit conditions, the settling time of the HRA is around 5.27s. This implies that HRA can tolerate up to four open circuits faults.

In general, equipping the track switch system with HRA can effectively improve its fault tolerance up to 4 actuator failures, on the premise that there is at least one healthy element in each series layer. The system's performance gradually declines depending on the number of failures of the sub-actuators. That is, it takes more time to meet the control requirements.

V. CONCLUSIONS

This paper is structured into three main parts: The first part starts with modelling of a single electro-mechanical actuator. Subsequently, the authors develop the rail model by Finite Element Analysis and testes against the experimental results from the Simpack model. After that, a switch model, including an HRA with nine element (three by three) actuators, is constructed form an HRA switch system. The application of HRA attempts to demonstrate the possibility of using mechanical structures to accommodate such failures in drive components. Finally, two closed-loop control methods are designed and applied for the track switch under healthy and faulty scenarios.

This is the first attempt in this field, which provides insight into the actuator fault-tolerant approach for the switch system to realise continuous operations and avoid unnecessary maintenance. A track switch system with a closed-loop controller has also not been applied in practice anywhere in the world. Hence this work will be of interest to global rail companies and could lead to potential collaborative links.

REFERENCES

[1] S. D. Bemment, R. M. Goodall, R. Dixon, and C. P. Ward, "Improving the reliability and availability of railway track switching by analysing historical failure data and introducing functionally redundant subsystems," Proceedings of the Institution of Mechanical Engineers, Part F: Journal of rail and rapid transit, vol. 232, no. 5, pp. 1407-1424, 2018.

[2] S. Bemment, R. Dixon, R. Goodall, and S. Brown, "Redundantly engineered track switching for enhanced railway nodal capacity," IFAC Proceedings Volumes, vol. 46, no. 25, pp. 25-30, 2013.
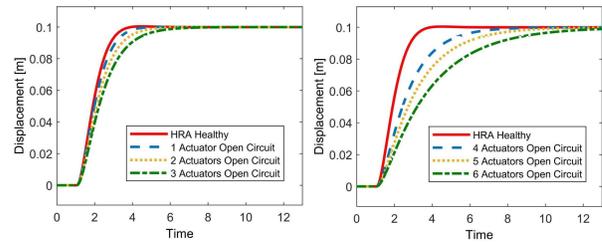
[3] P. L. Kaijuka, R. Dixon, C. P. Ward, S. Dutta, and S. Bemment, "Model-based controller design for a lift-and-drop railway track switch actuator," IEEE/ASME Transactions on Mechatronics, vol. 24, no. 5, pp. 2008-2018, 2019.

[4] J. Lee, H. Choi, D. Park, Y. Chung, H.-Y. Kim, and S. Yoon, "Fault detection and diagnosis of railway point machines by sound analysis," Sensors, vol. 16, no. 4, p. 549, 2016.

[5] Hamadache, M., et al., On the fault detection and diagnosis of railway switch and crossing systems: an overview. Applied Sciences, 2019. 9(23): p. 5129.

[6] M. Sarmiento-Carnevali, T. Harrison, S. Dutta, S. Bemment, C. Ward, and R. Dixon, "Design, construction, deployment and testing of a full-scale Repoint Light track switch (I)," 2017.

[7] X. Du, R. Dixon, R. M. Goodall, and A. C. Zolotas, "Modelling and control of a high redundancy actuator," Mechatronics, vol. 20, no. 1, pp. 102-112, 2010.

[8] G. Qiao, G. Liu, Z. Shi, Y. Wang, S. Ma, and T. C. Lim, "A review of electromechanical actuators for More/All Electric aircraft systems," Proceedings of the Institution of Mechanical Engineers, Part C: Journal of Mechanical Engineering Science, vol. 232, no. 22, pp. 4128-4151, 2018.

[9] R. Dixon et al., "Hra-intrinsically fault tolerant actuation through high redundancy," IFAC Proceedings Volumes, vol. 42, no. 8, pp. 1216-1221, 2009.

[10] H. Antong, R. Dixon, and C. P. Ward, "High Redundancy Actuator with 12 Elements: Open-and Closed-loop Model Validation," IFAC-PapersOnLine, vol. 49, no. 21, pp. 254-259, 2016.

[11] Biju, N. and R.P. MR, High redundancy electromechanical actuator for thrust vector control of a launch vehicle. Aircraft Engineering and Aerospace Technology, 2019.

[12] S. Dutta, T. Harrison, C. P. Ward, R. Dixon, and T. Scott, "A new approach to railway track switch actuation: Dynamic simulation and control of a self-adjusting switch," Proceedings of the Institution of Mechanical Engineers, Part F: Journal of Rail and Rapid Transit, vol. 234, no. 7, pp. 779-790, 2020.

[13] L. Li, S. Dutta, R. Dixon and E Stewart, "Modeling a track switch - Development and validation of a finite element solution," Proceedings of the Institution of Mechanical Engineers, Part F: Journal of Rail and Rapid Transit, submitted for publication.

[14] S. R. Gunakala, D. Comissiong, K. Jordan, and A. Sankar, "A finite element solution of the beam equation via MATLAB," International Journal of Applied, vol. 2, no. 8, 2012.

[15] X. Ling and A. Haldar, "Element level system identification with unknown input with Rayleigh damping," Journal of Engineering Mechanics, vol. 130, no. 8, pp. 877-885, 2004.

[16] H. Panzer, J. Hubele, R. Eid, and B. Lohmann, "Generating a parametric finite element model of a 3d cantilever timoshenko beam using matlab," Lehrstuhl für Regelungstechnik, 2009.

[17] P. Dash, L. C. Saikia, and N. Sinha, "Automatic generation control of multi area thermal system using Bat algorithm optimized PD–PID cascade controller," International Journal of Electrical Power Energy Systems, vol. 68, pp. 364-372, 2015.

[18] A. Saleem, B. Taha, T. Tutunji, and A. Al-Qaisia, "Identification and cascade control of servo-pneumatic system using particle swarm optimization," Simulation Modelling Practice and Theory, vol. 52, pp. 164-179, 2015.

[19] Y. Lee, S. Park, and M. Lee, "PID controller tuning to obtain desired closed loop responses for cascade control systems," Industrial engineering chemistry research, vol. 37, no. 5, pp. 1859-1865, 1998.